

# Role of CO<sub>2</sub> in the formation of gold deposits

G. N. Phillips<sup>1</sup> & K. A. Evans<sup>2</sup>

<sup>1</sup>CSIRO Division of Exploration and Mining, PO Box 3, Central Park, Victoria 3145, Australia

<sup>2</sup>CSIRO Division of Exploration and Mining, School of Geosciences, Building 28, Monash University, Victoria 3800, Australia

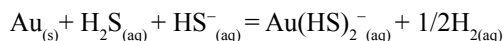
**Much of global gold production has come from deposits with uneconomic concentrations of base metals, such as copper, lead and zinc<sup>1</sup>. These 'gold-only' deposits are thought to have formed from hot, aqueous fluids rich in carbon dioxide<sup>2</sup>, but only minor significance has been attached to the role of the CO<sub>2</sub> in the process of gold transport. This is because chemical bonding between gold ions and CO<sub>2</sub> species is not strong<sup>3</sup>, and so it is unlikely that CO<sub>2</sub> has a direct role in gold transport. An alternative indirect role for CO<sub>2</sub> as a weak acid that buffers pH has also appeared unlikely, because previously inferred pH values for such gold-bearing fluids are variable<sup>2,4,5,6</sup>. Here we show that such calculated pH values are unlikely to record conditions of gold transport, and propose that CO<sub>2</sub> may play a critical role during gold transport by buffering the fluid in a pH range where elevated gold concentration can be maintained by complexation with reduced sulphur. Our conclusions, which are supported by geochemical modelling, may provide a platform for new gold exploration methods.**

The world's major gold-only deposits have formed by precipitation of gold from aqueous fluids migrating on a kilometre-scale through the bedrock that comprises the upper part of the Earth's crust. These fluids show a remarkably consistent set of characteristics. They are at temperatures above 200 °C, rich in CO<sub>2</sub> (up to 20–30 mol%; Table 1), sulphur-bearing, low salinity compared to most ore-bearing fluids, and have a redox state more reducing than the haematite–magnetite buffer such that the sulphur is predominantly in the reduced state<sup>1</sup>. These characteristics have been confirmed (by techniques including fluid-inclusion and stable-isotope analyses) for deposit types that account for the bulk of the world's gold production, both today and historically—for example, Archaean greenstone gold<sup>2,7</sup>, slate-belt gold<sup>8</sup>, the Mother Lode of California<sup>6</sup>, gold in banded iron formations<sup>2</sup>, Carlin-type gold<sup>9</sup> and the Witwatersrand goldfields<sup>9,10</sup>.

With the exception of the high CO<sub>2</sub> concentrations, these shared fluid characteristics can be explained by the chemical attributes of the dissolved gold. The somewhat reducing fluids and elevated temperatures favour the ionic state of Au<sup>+</sup> for the gold in solution<sup>3</sup>. Au<sup>+</sup> is the softest of cations, that is, it prefers covalent bonding<sup>3,11,12</sup>. Soft cations preferentially bond with soft anions and ligands, so Au<sup>+</sup> forms strong complexes with soft ligands. HS<sup>-</sup> is one of the few ligand candidates to meet the dual criteria

of being moderately abundant in these fluids, and soft in character. Hydrosulphide complexing of gold is consistent with laboratory experiments<sup>13</sup>, with inferred sulphidation and redox depositional mechanisms in the formation of gold deposits<sup>11,14</sup>, and with the abundance of sulphide minerals (such as pyrite) in gold deposits. Hydrosulphide complexing of gold is also consistent with low salinities. Chlorine forms a moderately hard anion (Cl<sup>-</sup>), and although it can complex with gold under oxidizing conditions, under the more reducing conditions inferred for gold-only deposits, it bonds preferentially with harder cations, such as Cu, Pb and Zn. Low salinities and a lack of these base metals in gold-only deposits are thus consistent with hydrosulphide complexing.

To understand the role of the CO<sub>2</sub>, it is necessary to examine interactions between sulphur complexation and other fluid constituents during gold transport and deposition. The concentration of gold in potentially ore-forming solutions is a function of the distribution of sulphur species. For temperatures of 200–400 °C, pressures of 200 MPa and near-neutral pH, Au(HS)<sub>2</sub><sup>-</sup> is the dominant gold–hydrosulphide complex<sup>15</sup>. Gold concentrations can be related to those of the sulphide species via:



$K$ , the stability constant, is defined by:

$$K = \frac{\{Au(HS)_2^-\} \{H_2\}^{0.5}}{\{H_2S\} \{HS^-\}}$$

where {...} indicates activity. This can be rearranged to give  $\{Au(HS)_2^-\}$ , the gold activity in solution:

$$\{Au(HS)_2^-\} = \frac{K \{H_2S\} \{HS^-\}}{\{H_2\}^{0.5}}$$

The maximum gold solubility at a given hydrogen activity occurs when the product  $\{H_2S\} \{HS^-\}$  is maximized, and as these sulphur species are related by  $H_2S \leftrightarrow HS^- + H^+$ , the maximum occurs when  $\{H_2S\} = \{HS^-\}$ . For  $K_1(H_2S) = \{HS^-\} \{H^+\} / \{H_2S\} = \{H^+\}$ , it follows that the maximum occurs where  $pH = pK_1(H_2S)$ .

With respect to pH and redox parameters, the maximum gold solubility occurs close to the point where hydrogen sulphide, bisulphide and sulphate species coexist in equal quantities. The redox state must be largely wallrock-controlled<sup>14</sup>, because the fluid has a low redox buffering capacity. However, further information is required to determine whether pH is controlled by fluid or wallrock. Two lines of evidence suggest that pH during gold transport is fluid-buffered. First, in the strongly altered wallrocks typical of goldfield environments, mineral buffers of pH are often exhausted<sup>14,16</sup>, suggesting that pH was controlled by components within the fluid. Second, pH changes are not usually implicated as the main control on gold deposition, indicating that pH in the fluid was largely independent of wallrock.

We propose that CO<sub>2</sub> within the fluid provided the buffering capacity needed to maintain elevated gold solubilities. A pH buffer needs to be both abundant and to have weak acid–base properties. H<sub>2</sub>CO<sub>3</sub> is a weak acid that is abundant

in the gold-bearing fluid (up to 200,000–300,000 p.p.m. total for all carbon species), and has pH buffering capability through  $\text{H}_2\text{CO}_3 = \text{HCO}_3^- + \text{H}^+$  relationships. Importantly, the first dissociation constant for  $\text{H}_2\text{CO}_3$  is close to the first dissociation constant of  $\text{H}_2\text{S}$  for a range of geologically relevant temperatures (Fig. 1a). We have already shown that maximum gold solubility occurs where the pH equals  $\text{p}K_1(\text{H}_2\text{S})$  for any given hydrogen activity, so that a fluid experiencing a significant degree of  $\text{CO}_2$  buffering near  $\text{p}K_1(\text{H}_2\text{CO}_3)$  would automatically be maintained in a region of elevated gold solubility.

Two issues militate against acceptance of this role for  $\text{CO}_2$ . The first is that published estimates of pH in auriferous fluids are highly variable, and often significantly different to  $\text{p}K_1$  for  $\text{CO}_2$  or  $\text{H}_2\text{S}$  (Table 1). This variability is incongruous with the remarkably consistent chemical characteristics of gold-only deposits<sup>1</sup>. These pH estimates rely on  $\text{K}^+/\text{H}^+$  and  $\text{Na}^+/\text{H}^+$  ratios derived from observed alteration mineral assemblages (for example, pyrophyllite plus muscovite), and, in some cases, measurement of the K/Na ratio in fluid inclusions. Such calculations of pH values are likely to be unreliable because extensive and widespread K and Na metasomatism observed in gold deposit wallrocks indicates that both elements are intimately involved in the depositional process. It is therefore likely that these pH values derived indirectly using measurements of Na and K relate to intermediate depositional processes rather than values during gold transport.

The second issue is based on the fact that in a pure C-O-H-S fluid, the only cation species would be  $\text{H}^+$ , and pH would be significantly below the  $\text{p}K_1$  for either  $\text{CO}_2$  or  $\text{H}_2\text{S}$ . Under these circumstances, both  $\text{H}_2\text{S}$  and  $\text{CO}_2$  would be almost fully associated, and could not buffer pH. However, ore-forming fluids interact with wallrocks as they travel through the Earth's crust, and  $\text{H}^+$  ions exchange for  $\text{Na}^+$  and  $\text{K}^+$  ions. Loss of  $\text{H}^+$  through this exchange increases the pH of the fluid to the vicinity of  $\text{p}K_1(\text{H}_2\text{CO}_3)$  for geologically reasonable  $\text{K}^+$  concentrations (Fig. 1b), so this issue is not an obstacle to the suggestion that  $\text{CO}_2$  buffers pH.

We have tested the hypothesis that  $\text{CO}_2$  buffering can control pH in gold-bearing fluids using the geochemical

modelling program HCh and its associated Unitherm database. These comprise a software package designed for equilibrium modelling of fluid–rock systems<sup>17</sup>. The chemical system modelled was K-Mg-Fe-Al-Ca-C-Si-H-O-Au-S, and the database includes  $\text{Au}^+$  and  $\text{Au}^{3+}$  hydroxides and hydrosulphides (see Methods section for full list). Chloride was not included because there is no evidence for geologically high salinity fluids in the deposits of interest (Table 1). A brief conceptual description of the model is given here, further details can be found in the Methods section.  $\text{H}_2\text{O}$ – $\text{CO}_2$  fluids with 10 mol%  $\text{CO}_2$  were initially equilibrated with a basalt at 200 MPa, 400 °C, and a fluid:rock ratio of 1:1. Equilibrated fluids were then added to the bottom of a modelled rock column (Fig. 1c). Each of the seven lithological units within the column is composed of 10 reacting cells; the fluid equilibrates with each cell before being passed on to the next. Fluid–rock ratios were set to 5:1 to mimic the focusing of fluids in ore-forming systems. Multiple waves of fluid passed up the hypothetical column; initial fluids for each wave were equilibrated with the gold-bearing basalt, as for the first step, but were then reacted with cells of rock that had already been modified by fluids from the preceding steps. Temperature was set to decrease by 3 °C per cell as the column was ascended. The redox state was set above the pyrrhotite–pyrite–magnetite buffer, such that neither methane nor sulphate were stable with respect to carbon dioxide and hydrogen sulphide, respectively. Results were compared with a control run with 0.1 mol%  $\text{CO}_2$ . The model is used to derive trends and relative, rather than absolute, values, because of inherent uncertainties in thermodynamic data and the limited applicability of the thermodynamic model to  $\text{CO}_2$ -rich solutions.

Selected results of the final wave of the model are shown in Fig. 1d–f, which illustrate pH, proportion of the sulphur as  $\text{HS}^-$  for  $\text{CO}_2$ -bearing and  $\text{CO}_2$ -free fluids, and gold concentration in the rock, respectively. pH in the  $\text{CO}_2$ -bearing fluid is lower than that of  $\text{CO}_2$ -free (Fig. 1d), because of the acidic nature of the  $\text{CO}_2$ . The  $\text{CO}_2$ -free fluid can carry more gold, but this is not a limiting factor at the source, as typical basaltic source rocks contain only a few p.p.b. of gold, and devolatilization results in gold undersaturated

**Table 1 Gold-related fluid characteristics from major ore deposits**

	$\text{CO}_2$ (mol%)	pH evidence	Inferred pH	Salinity (wt% NaCl eq.)
Witwatersrand <sup>4</sup>	NA	Pyrophyllite	Acid	NA
Witwatersrand <sup>25</sup>	NA	Muscovite	3.8–5	12
Vaal Reefs South, South Africa <sup>10</sup>	Significant	NA	NA	6–18
Archaean Greenstone (general) <sup>5</sup>	NA	Dolomite	Near neutral	NA
Hollinger mine, Canada <sup>7</sup>	10–20	NA	NA	Low to variable
Hunt, Kambalda <sup>2,14</sup>	25	Na/K	6.9	2
Slate Belt (general) <sup>25</sup>	NA	Calcite	Near-neutral	NA
Wattle Gully, Castlemaine, Victoria <sup>8</sup>	20	NA	NA	Low
Carlin deposit, Nevada, USA <sup>9</sup>	5–10	NA	NA	3
Mother Lode, California <sup>6</sup>	10	Na/K	6	3

Fluid compositions refer to the majority of recorded fluids, rather than to the full range. Gold deposits with economic base metals may have salinities of 50 wt% NaCl equivalent or greater<sup>26,27</sup>. NA, not available.

solutions over a wide range of temperature. Changes in sulphur species distribution (Fig. 1e) are almost eliminated in the CO<sub>2</sub>-bearing fluid, providing a stable chemical environment for gold transport through the Earth's crust. Modelled mineral abundances (not shown) indicate that CO<sub>2</sub>-bearing and CO<sub>2</sub>-free fluids will deposit gold in basalt as a result of pyrite-forming reactions between sulphur in the fluid, and iron within the rock. This mechanism is important in gold deposits<sup>14</sup>, and its occurrence here supports the CO<sub>2</sub> buffering hypothesis.

A significant difference between the two hypothetical fluids lies in the distribution of deposited Au (Fig. 1f). The CO<sub>2</sub>-bearing fluid focuses gold deposition over a narrow distance and temperature range, whereas the CO<sub>2</sub>-free fluid deposits gold over a greater distance but at lower concentrations. The former is more likely to result in an economic gold deposit. The contrasting deposition pattern results from CO<sub>2</sub> buffering pH to lower levels as temperature decreases (Fig. 1d), leading to a greater deposition of Au when suitable rock types (for example, Fe-rich basalts) are encountered. The difference between CO<sub>2</sub>-bearing and CO<sub>2</sub>-free fluids is enhanced by a basalt-induced pH increase in the CO<sub>2</sub>-free fluid. The increase enhances gold solubility, reducing deposition by sulphidation, whereas the CO<sub>2</sub>-bearing fluid is buffered and so does not experience this pH increase, and deposits a greater proportion of the dissolved gold.

Our arguments do not incorporate the potentially significant effects of CO<sub>2</sub> on hydrogen-bonding in water and consequent changes in ion hydration, complex stability, mineral solubility and aqueous speciation<sup>18</sup>. Neither do we consider the effect of H<sub>2</sub>O–CO<sub>2</sub> immiscibility; this may be important in gold deposition, but is unlikely to play a significant role in transport.

To summarize, the role of CO<sub>2</sub> has commonly been regarded as peripheral because carbonate alteration and economic gold are only approximately coincident, and theory does not suggest gold complexing with the hard carbonate ligand. We suggest that CO<sub>2</sub> is essential in the formation of gold-only provinces and deposits, via its abilities to buffer fluid pH at a level that can maintain elevated concentrations of gold in solution, and allow gold deposition in chemically favourable host rocks. Previous estimates of the pH of gold-bearing fluids are likely to reflect transient depositional processes rather than the gold-transporting stage.

Our results have important implications for gold exploration. Process-based genetic models for gold deposits have already proved useful in the Yandal gold province of Western Australia, where 10 million ounces of Au have been discovered since 1990<sup>19</sup>. Better genetic models will help prioritize exploration parameters. Here we show that effective Au transport requires both H<sub>2</sub>S and CO<sub>2</sub>, which must, implicitly, be incorporated at the source of the Au, constraining the genesis of ore-bearing fluids. Characteristics determined at the source will be consistent throughout a group of gold deposits, for example, Yandal gold province, whereas those related to depositional site, such as high iron or carbon content, will account for some of the variability between deposits.

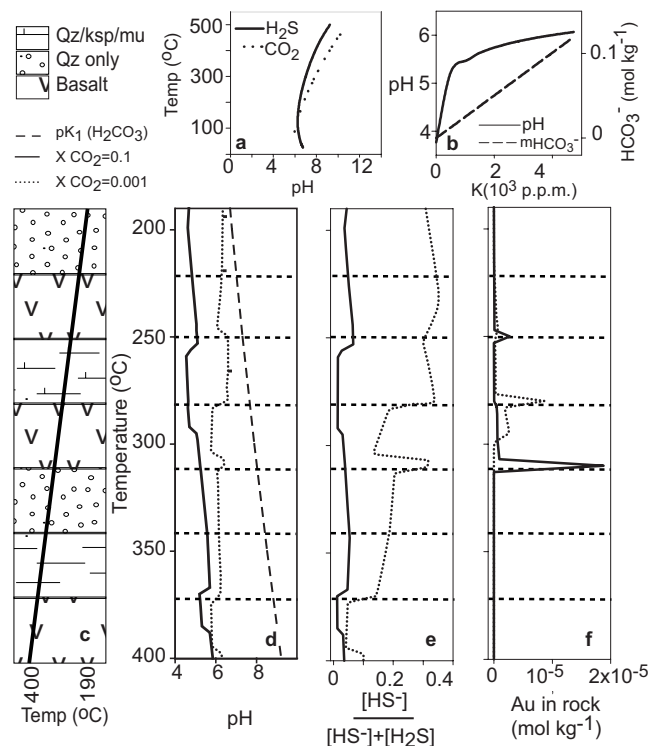


**Figure 1** Results of HCh modelling in the K-Fe-Mg-Ca-Al-Si-C-H-Au-S-O system. All figures are constructed using HCh and the Unitherm database. Pressure is 200 MPa in all cases. Qz, quartz; mu, muscovite; ksp, K-feldspar. **a**, Temperature–pH plot showing  $pK_1$  for weak acids H<sub>2</sub>S and H<sub>2</sub>CO<sub>3</sub>.  $pK_1$  for H<sub>2</sub>CO<sub>3</sub> is very close to  $pK_1$  of H<sub>2</sub>S for a wide range of geological temperatures. Maximum gold solubility occurs along the H<sub>2</sub>S line. **b**, pH–[K] plot for a H<sub>2</sub>O–CO<sub>2</sub> fluid (15 mol % CO<sub>2</sub>) at 350 °C and 200 MPa.  $m_{\text{HCO}_3^-}$  is the molality of the HCO<sub>3</sub><sup>-</sup> ion. Without K, a fluid in this system is quite acid, but for K-present conditions, as implicated in the formation of gold deposits, the pH is much closer to  $pK_1(\text{H}_2\text{S})$ . The concentration of HCO<sub>3</sub><sup>-</sup>, and hence the buffering capacity of the fluid, have a positive correlation with the K concentration. **c**, Sequence of rock types used for the flow-through reactor modelling shown in **d–f**. Fluids equilibrate with a gold and sulphur-bearing basalt (not shown), and then cool from 400 °C to 190 °C as they pass upwards through successive rock types. Time-integrated fluid:rock ratios by weight are 50. **d–f**, Results of flow-through reactor modelling. Solid line, 10 mol % CO<sub>2</sub>; dotted line, 0.1 mol % CO<sub>2</sub>. **d**, pH of the modelled fluids as they progress through the rock sequence. The pH of the CO<sub>2</sub>-bearing fluid (initially 10 mol % CO<sub>2</sub>) decreases with temperature and is virtually parallel to the dashed line which shows  $pK_1(\text{H}_2\text{CO}_3)$ . The pH of the essentially CO<sub>2</sub>-free fluid (initially 0.1 mol % CO<sub>2</sub>) diverges markedly from the trend of  $pK_1(\text{H}_2\text{CO}_3)$ . Steps in pH indicate the positions of reaction fronts in the wallrocks. **e**, Proportion of the sulphur as HS<sup>-</sup> (defined as  $[\text{HS}^-]/([\text{HS}^-] + [\text{H}_2\text{S}])$ ). In the CO<sub>2</sub>-bearing fluid there are small changes related to changes of pH in **d**. The proportion of HS<sup>-</sup> is relatively constant because of the CO<sub>2</sub>-buffering of pH. This is strong confirmation that pH buffering by CO<sub>2</sub> controls the distribution of sulphur species. For the low CO<sub>2</sub> fluid, the proportion of HS<sup>-</sup> increases with decreasing temperature reflecting the divergence from  $pK_1(\text{H}_2\text{CO}_3)$  in **d**. Total reduced sulphur concentrations in both cases range from 20 mM at the base of the column to 0.01 mM at the top. **f**, Gold deposited from the fluids modelled in **c** and **d**. The CO<sub>2</sub>-bearing fluid deposits the gold in a more focused way in the Fe-rich basalt in response to sulphidation reactions. The CO<sub>2</sub>-poor fluid deposits gold over a broader part of the column.

## Methods

### HCh description

The HCh program package was developed for geochemical modelling of rock–fluid systems at moderate to high temperatures (1,000 °C) and moderate pressures (<500 MPa). It includes several programs that interact to calculate equilibrium compositions of multi-phase chemical systems using free-energy minimization techniques, and a thermodynamic database (Unitherm). This database, although carefully compiled, is taken from a variety of sources and is not internally consistent; however, observed compositional trends and comparisons are likely to be valid. Free energies of solid phases are calculated conventionally using reference entropies, enthalpies and volumes, with a Maier-Kelley expression for heat capacity<sup>17</sup>. Molar volumes of solids are assumed to be independent of pressure. The properties of pure water are calculated using the Haar-Gallager-Kell model<sup>20</sup>. Properties of selected aqueous endmembers (primary species) are calculated via the revised Helgeson-Kirkham-Flowers equations of state<sup>21,22</sup>. Other endmembers (secondary species) were calculated using values for the primary species and the modified Ryzhenko-Bryzgalin model<sup>17</sup>. Apparent molal standard state Gibbs free energies at the pressure and temperature of interest, calculated by Unitherm, are given in Supplementary Table M1 for the principal aqueous species involved in reactions plus additional gold species. The standard state for aqueous species is unit activity in an ideal hypothetical 1 molal solution at the pressure and temperature of interest, referenced to infinite dilution. The standard state for solid phases and water is unit activity for the pure phase at the pressure and temperature of interest. Solid phases were assumed to be pure endmembers. Activity coefficients of aqueous charged species were calculated using the extended Debye-Huckel equation. Extended term parameters are available for a variety of background electrolytes<sup>23,24</sup>. Neutral aqueous species were considered to mix ideally. The validity of the activity model is restricted to ionic strengths of less than 0.1; our modelled ionic strengths reach 0.14 at low temperatures, but are generally below 0.1. A greater concern results from the limited ability of the thermodynamic formulation to fully incorporate the effects of high CO<sub>2</sub> concentrations.

### Modelled system

Modelling was performed within the system K-Fe-Mg-Al-Si-C-Ca-H-O-Au-S. Bulk compositions for the rock types described in the text are given in Supplementary Table M2. Rock compositions present are basalt, aluminous psammite and pure quartz. These rock compositions reflect those present in the Eastern Goldfields of Australia. High SiO<sub>2</sub> values in Supplementary Table M2 are artefacts of the normalization scheme used. Quartz is in excess in any case, and high values do not affect conclusions. Au contents were 100 p.p.b.; this is high, but did not lead to a Au-saturated fluid. Unitherm contains data for 71 potential mineral phases and 61 different aqueous species within this composition space. Aqueous gold-bearing species were Au<sup>+</sup>,

AuOH, Au(OH)<sub>2</sub><sup>-</sup>, AuHS, Au(HS)<sub>2</sub><sup>-</sup>, Au<sup>3+</sup> and Au<sub>2</sub>(HS)<sub>2</sub>S<sup>-</sup>. 15 of the 71 minerals were stable in at least one rock type during modelling. Mineral assemblages were consistent with those observed in gold-only deposits (Supplementary Table M3), given the limitations of bulk composition and constraints on mineral compositions. Various combinations of fluid:rock ratio and number of fluid waves were tested to assess the sensitivity of the model to the discretization scheme. Discretization affects the details, but not the overall trends and conclusions produced by the model. A fluid:rock ratio of 5:1 was chosen for the calculations shown in Fig. 1.

Received 8 January; accepted 10 May 2004; doi:10.1038/nature02644.

- Phillips, G. N. & Powell, R. Link between gold provinces. *Econ. Geol.* **88**, 1084–1098 (1993).
- Ho, S. E., Groves, D. I. & Phillips, G. N. Fluid inclusions as indicators of the nature and source of ore fluids and ore depositional conditions for Archaean gold deposits of the Yilgarn Block, Western Australia. *Trans. Geol. Soc. S. Afr.* **88**, 149–158 (1985).
- Puddephatt, R. J. *The Chemistry of Gold* (Elsevier, Amsterdam, 1978).
- Barnicoat, A. C. *et al.* Hydrothermal gold mineralization in the Witwatersrand basin. *Nature* **386**, 820–824 (1997).
- Morrison, G. W., Rose, W. J. & Jaireth, S. Geological and geochemical controls on the silver content (fineness) of gold in gold-silver deposits. *Ore Geol. Rev.* **6**, 333–364 (1991).
- Bohlke, J. K. Comparison of metasomatic reactions between a common CO<sub>2</sub>-rich vein fluid and diverse wall rocks: intensive variables, mass transfers, and Au mineralization at Alleghany, California. *Econ. Geol.* **84**, 291–327 (1989).
- Smith, T. J., Cloke, P. L. & Kesler, S. E. Geochemistry of fluid inclusions from the McIntyre-Hollinger gold deposit, Timmins, Ontario. *Econ. Geol.* **79**, 1265–1285 (1984).
- Cox, S. F., Wall, V. J., Etheridge, M. A. & Potter, T. F. Deformational and metamorphic processes in the formation of mesothermal vein-hosted gold deposits — examples from the Lachlan Fold Belt in central Victoria, Australia. *Ore Geol. Rev.* **6**, 391–423 (1991).
- Kuehn, C. A. & Rose, A. W. Carlin gold deposits, Nevada: origin in a deep zone of mixing between normally pressured and overpressured fluids. *Econ. Geol.* **90**, 17–36 (1995).
- Phillips, G. N., Klemd, R. & Robertson, N. S. Summary of some fluid inclusion data from the Witwatersrand Basin and surrounding granitoids. *Mem. Geol. Soc. India* **11**, 59–65 (1988).
- Phillips, G. N. & Groves, D. I. The nature of Archaean gold-bearing fluids as deduced from gold deposits of Western Australia. *J. Geol. Soc. Austr.* **30**, 25–39 (1983).
- Ahrland, S., Chatt, J. & Davies, N.R. The relative affinities of ligand atoms for acceptor molecules and ions. *Q. Rev. Chem. Soc.* **12**, 265–276 (1958).
- Seward, T. M. Thio-complexes of gold in hydrothermal ore solutions. *Geochim. Cosmochim. Acta* **37**, 379–399 (1973).
- Neall, F. B. & Phillips, G. N. Fluid-wall interaction in an Archaean hydrothermal gold deposit: a thermodynamic model for the Hunt Mine, Kambalda. *Econ. Geol.* **82**, 1679–1694 (1987).
- Benning, L. G. & Seward, T. M. Hydrosulphide complexing of Au(I) in hydrothermal solutions from 150–400 degrees C and 500–1500 bar. *Geochim. Cosmochim. Acta* **60**, 1849–1871 (1996).

16. Phillips, G. N. & Law, J. D. M. Witwatersrand gold fields: geology, genesis and exploration. *SEG Rev.* **13**, 439–500 (2000).
17. Shvarov, Y. & Bastrakov, E. *HCh: A Software Package for Geochemical Equilibrium Modelling. User's Guide* (Record 1999/25, Australian Geological Survey Organisation, 1999).
18. Gibert, F., Moine, B., Schott, J. & Dandurand, J.-L. Modelling of the transport and deposition of tungsten in the scheelite-bearing calc-silicate gneisses of the Montagne Noire, France. *Contrib. Mineral. Petrol.* **112**, 371–384 (1992).
19. Phillips, G. N. & Vearncombe, J. R. Exploration of the Yandal gold province, Yilgarn Craton, Western Australia. *CSIRO Explores* **1**, 1–26 (2003).
20. Kestin, J., Sengers, J. V., Kamgar-Parsi, B. & Levelt Sengers, J. M. H. Thermophysical properties of fluid H<sub>2</sub>O. *J. Phys. Chem. Ref. Data* **13**, 175–183 (1984).
21. Tanger, J. C. & Helgeson, H. C. Calculation of the thermodynamic and transport-properties of aqueous species at high-pressures and temperatures — revised equations of state for the standard partial molal properties of ions and electrolytes. *Am. J. Sci.* **288**, 19–98 (1988).
22. Shock, E. L., Oelkers, E. H., Johnson, J. W., Sverjensky, D. A. & Helgeson, H. C. Calculation of the thermodynamic properties of aqueous species at high pressures and temperatures. *J. Chem. Soc. Faraday Trans.* **88**, 803–826 (1992).
23. Helgeson, H. C., Kirkham, D. H. & Flowers, G. C. Theoretical prediction of the thermodynamic behaviour of aqueous electrolytes at high pressures and temperatures: IV Calculation of activity coefficients, osmotic coefficients, and apparent molal and standard and relative partial molal properties to 600 degrees C and 5 kbar. *Am. J. Sci.* **281**, 1259–1516 (1981).
24. Oelkers, E. H. & Helgeson, H. C. Triple-ion anions and polynuclear complexing in supercritical electrolyte-solutions. *Geochim. Cosmochim. Acta* **54**, 727–738 (1990).
25. Robb, L. J. & Meyer, F. M. A contribution to recent debate concerning epigenetic versus syngenetic mineralization processes in the Witwatersrand basin. *Econ. Geol.* **86**, 396–401 (1991).
26. Eastoe, C. J. A fluid inclusion study of Panguna porphyry copper deposit, Bougainville, Papua New Guinea. *Econ. Geol.* **73**, 721–748 (1978).
27. Goellnicht, N. M., Groves, D. I., McNaughton, N. J. & Dimo, G. An epigenetic origin for the Telfer gold deposit. *Econ. Geol. Monogr.* **6**, 151–167 (1989).

Supplementary Information accompanies the paper on [www.nature.com/nature](http://www.nature.com/nature).

**Acknowledgements** We thank J. Law and M. Hughes for critical comments; R. Smith for earlier discussions relating to the chemical behaviour of gold; and R. Phillips and S. Wood for comments and suggestions that helped to improve the manuscript. K.A.E. acknowledges honorary positions at Monash and Melbourne Universities.

**Competing interests statement** The authors declare that they have no competing financial interests.

**Correspondence** and requests for materials should be addressed to G.N.P. ([neil.phillips@csiro.au](mailto:neil.phillips@csiro.au)).